Process and Materials Development for Functionalized Printing in Three Dimensions (FP-3D)

D. Polsakiewicz, W. Kollenberg

The paper presents the development pathway for the generation of ceramic parts with locally changed materials compositions. Focussing on the issues of ink preparation and characterization, the local doping of ceramic powder through printing in former publications hence establishing valuable building blocks in process development, this paper focusses on particle filled ink printing and powder selection for the process. The Ohnesorge number is confirmed as a good indicator for ink printability, but final printing settings also have to be verified by direct observation of the drop formation process before fabrication. Powder investigations revealed that particle packing models for coarse powders are not valid for fine powders used here and desired for the process. But without embedding the process into powder analysis, final conclusions do not seem possible. Hence, the development of suitable methods for this particular question is the focus of present and future research.

1 Introduction

During the development of new materials, often the experimental procedure is designed to match the industrial fabrication in order to ensure good compatibility of newly developed materials with existing processing and fabrication technologies. But for understanding general effects and phenomena for ceramic structures without considering a specific fabrication process, general investigations on many materials without changing the fabrication process seem very interesting in order to investigate generalized effects. In the field of refractories for example, few publications deal with the development of model refractory materials in order to provide opportunities for the investigation of generalized effects in refractory microstructures [1]. With knowledge of those effects, materials could be tailored to specific needs derived from the model systems applied in general investigations. By leaving classic processing approaches in materials development, also a closer look at different materials systems not yet considered for specific applications seems possible without taking processing aspects into account. For example, the reduction or avoidance of carbon content in refractory materials has been a focus of the industry in recent years due to the need for environmentally clean materials and the research for carbon-free alternatives in refractory applications has intensified in Germany over the past few years [2]. In the context of the search for new approaches to materials design, research for flexible and multi-material processing methods has been initiated and conducted at the University of Applied Sciences Bonn-Rhine-Sieg.

Dominik Polsakiewicz,
Wolfgang Kollenberg
Hochschule Bonn-Rhein-Sieg
53359 Rheinbach
Germany

Corresponding-Author:
Dominik Polsakiewicz
E-mail: dominik.polsakiewicz@h-brs.de

Keywords: 3D-printing, alumina, generative manufacturing

Received: 11.10.2011
Accepted: 24.10.2011

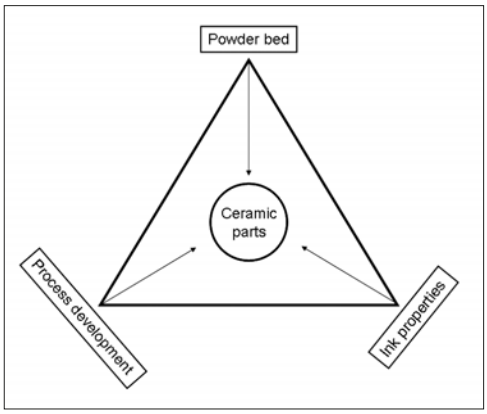

Fig. 1 Development strategy for the realization of Functionalized Printing in Three Dimensions (FP-3D)

Starting point for the research was a newly developed fabrication method for ceramic structures based on prototyping technologies and inkjet printing [3] which is supposed to be realized by the build-up of an experimental platform in order to understand the influence of various process variables and their influence on fabricated structures. Three main aspects identified as necessary for a successful realization of this experimental procedure are shortly illustrated in Fig. 1.

In former publications from this research project, the generation of graded structures through particle-filled inks printed into a powder bed of a few powder layers have been successfully reported. Fig. 2 and 3 show an alumina ceramic powder compact of a few layers (up to 5) modified with an ink containing zirconia, Fig. 5 and 4 illustrate a structure doped with zirconia in a graduated fashion [4].

Further work demonstrated first structures of alumina powder containing silica-based inks printed into parts of 10 layers or more [5],

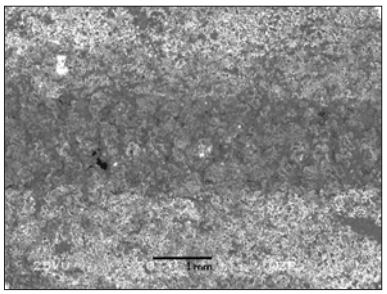

Fig. 2 Alumina powder compact printed with three zones of zirconia ink (BSE-SEM)

Fig. 3 EDX analysis corresponing to Fig. 2 (Zr: grey)

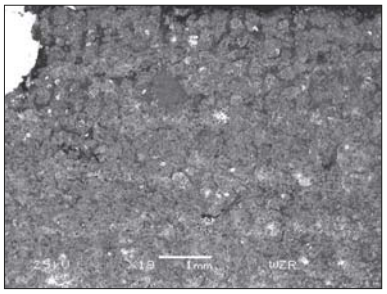

Fig. 4 Alumina powder compact printed with zirconia in a graded profile (BSE-SEM)

Fig. 5 EDX analysis corresponding to Fig. 5 (Zr: grey)

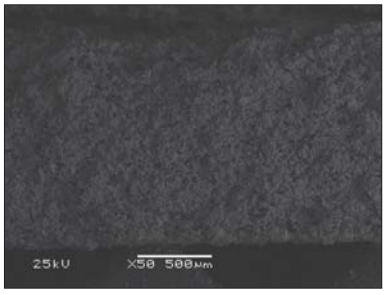

Fig. 6 Alumina ceramic with Si ink printed in ceramic body (BSE-SEM)

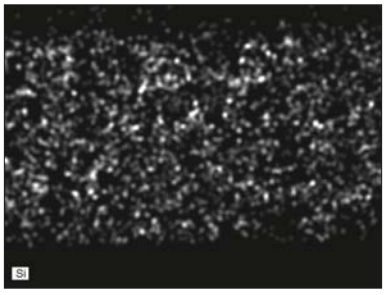

Fig. 7 EDX analysis corresponding to Fig. 6 (Si: white)

revealing the need for improvement regarding the strength and mechanical stability of the generated parts thus showing the opportunities for manipulating structures even in three dimensions. An example for a structure is given in Fig. 6 and 7.

Investigations of inks prepared for the printing process also have been reported revealing the need for printing experiments with such inks in order to fully understand their capability for the desired utilization [6]. In the following paper, the two main focusses are for one identifying suitable printing parameters for newly prepared inks as well as ink characterization and observation of printing performance, on the other hand powder compacts mixed from different raw materials with differing sizes and shapes are investigated in order analyse the theoretical potential of such powder mixtures for the build-up of ceramic structures. First demonstration parts fabricated from selected powders are presented as well.

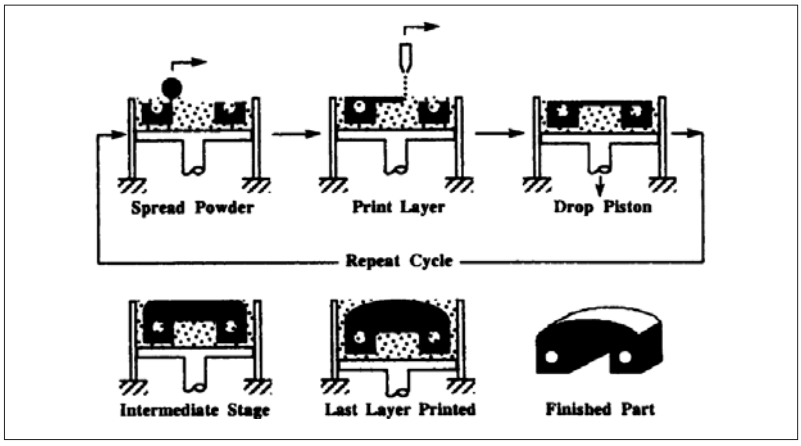

Fig. 8 Basis process steps for classic 3DP [8]

2 Experimental

2.1 Realization of experimental platform for FP-3D

The classic approach to 3D-Printing (3DP), already applied in commercially available machines and investigated by numerous researchers (an introductory overview is given in [7]) was taken as a basic principle in the conception of the newly developed experimental platform. The principle with its basic steps is illustrated in Fig. 8. In order to increase the flexibility of the machine regarding process able powders and inks, two main modifications were constructed compared to most commercially available printers for 3DP. First, the creation of powder layers was modified compared to most available systems. In most commercial machines the building area is accompanied by a feeding reservoir of the same dimensions placed directly next to the printing plane. While for each new layer the building area is lowered by a defined layer height, the feeding area is raised by the same amount. A doctor roller then removes the overlaying powder from the feeding to the building area.

For the experimental platform (FuGeMa 1.0 = Functionalized Generative Manufacturing platform Version 1.0) here, the powder for generation of new layers is placed in a storage container mounted on an axis separate from the printing station. For a new powder layer the container is placed above the building area (100 mm × 100 mm) and powder is placed into a void created by lowering the already printed layers. Metering of powder is realized through vibratory forces, a simple method which is stated to lack great disadvantages according to a review by *Yung* [9]. Additionally, vibratory

forces can help overcome interior friction in powder compacts thus opening up possibilities for the generation of higher packing densities in the resulting powder bed. The necessary vibrations are created by an unbalance motor (up to 40 000 rpm), transferred to the powder reservoir causing the powder to flow through an orifice. A shutter determines the areas where powder is coated onto the existing powder bed. A doctor roller made of polished stainless steel following the powder coater can be rotated clock- or counter-clockwise in order to smooth or/and compact the prepared powder layer surface and to remove excessive powder from the printing area. Direction, speed and diameter of the roller can be adjusted as needed. The aim was to obtain the possibility of metering even fine powders with restricted flowability during the coating process. Like in most 3DP machines, the powder bed is lowered by a lifting unit accordingly to the set layer thickness, which can be varied in steps of 10 µm.

The second main aspect differing from most 3DP machines is the use of piezoelectric driven single-nozzle print heads instead of thermal multi-nozzle print heads. The use of single-nozzle heads is reported for the fabrication of ceramic structures through Direct Ceramic Ink-Jet Printing, where a part is build-up directly on a substrate without a powder bed. This approach is often used for the fabrication of small parts compared to classic 3DP [10–12]. The print heads used in this study (microdrop MK-140, *microdrop Technologies/DE*) provide an adjustable rectangular driving signal for droplet generation. Height and width of the signal can be adjusted in the range of 0 to 255 V and 0 to 255 µs, respectively. The print heads used have an orifice diameter of 100 µm which can be heated up to 60 °C. Due to the horizontal orientation of the nozzle orifice as well as the ink chamber, which are not separated by an additional channel, an under-pressure must be applied to the print head in order to prevent the ink from dripping out of the orifice. This under-pressure can be varied from 0 to –30 mbar. Visualization of droplet formation is realized through a CCD camera equipped with a strobe diode. The diode is synchronized with the drop generation frequency and therefore droplet formation can be visualized before printing. The intended advantage through the use of mentioned print heads is for one the ability to study the drop formation process for inks prepared with new raw materials and differing properties. On the other hand droplet ejection can be modified by adjusting the driving signal, a possibility not existent for thermally driven print heads.

The data for part fabrication is delivered in paths in contrast to many printing units, especially multi-nozzle systems, where the printed structures are provided in a grid pattern. The parts are generated from single monochrome or coloured pictures. Each picture represents a layer in the final part; each colour is reserved for a specific print head. For each layer, the distance from print head to powder bed, the line spacing between two lines as well as the distance between two droplets placed along a path is adjustable in multiples of 10 µm.

FuGeMa 1.0 possesses numerous adjustable parameters allowing experiments with a large variety of set-ups.

2.2 Ink preparation and characterization

Ink selection and investigation for alumina inks with tailored properties containing micron alumina powders for the specific print heads used in FuGeMa 1.0 has already been partially reported elsewhere [6]. The experiments presented here concentrate on a selection of inks filled with particles ranging in the nano-scale.

Three different inks were selected to act as examples for various possible inks and combinations of those. One alumina ink (further called ink A), one silica ink (further called ink S) and an ink with mullite composition (79 mass-% Al_2O_3 and 21 mass-% SiO_2, further called ink AS) were characterized for this paper.

As raw materials, a commercially available suspension of fumed silica (VP Disp W 1450, *Evonik/DE*), an alumina powder (AluC, *Evonik/DE*) and a powder of amorphous silica (Ox 50, *Evonik/DE*) were used.

Inks were prepared by mixing a polymeric dispersing agent (Solsperse 41090, *Lubrizol/UK*) into water and then adding the powder to the solvent system. The prepared ink was homogenized in the ball mill for 24 h.

After preparation, viscosity, surface tension and density of the inks were measured.

Viscosity was measured using a rotational viscosimeter (Bohlin CVO, *Malvern Instruments/UK*) with a cone-plate geometry. The cone had a diameter of 40 mm and an angle of 4°. The viscosity was analyzed in a shear rate range of 1 to 1000 s^{-1} at 25 °C.

Surface tension was investigated using a bubble lifetime tensiometer (SITA Pro line t15, *SITA Messtechnik/DE*) with a constant bubble lifetime of 0,5 s as well as over the bubble lifetime range from 15 ms to 15 000 ms. Density was measures by weighing a defined volume of ink (500 µl) on a precision scale.

The Ohnesorge number (Oh) was calculated from the measured properties in order to determine the printability of the prepared inks. The Ohnesorge number was calculated according to equation 1. For the calculations, the viscosity at a shear rate of 1000 s^{-1}, the surface tension for a bubble lifetime of 0,5 s and the measured density were used.

$$Oh = \frac{\mathrm{Re}^{1/2}}{We} = \frac{\eta}{\sqrt{(\sigma \rho a)}} \quad (1)$$

η: viscosity
σ: surface tension
ρ: density
a: characteristic length scale (nozzle orifice)

2.3 Investigation of powder mixtures for FP-3D

In order to determine a suitable powder composition for the powder bed, different alumina powders mixed with a polymeric binder and their comparative characteristics were investigated.

As raw materials, a tabular alumina (T 60, *Almatis/DE*; further referred to as powder C1) and a granulated alumina (Martoxid MR 70/S, *Martinswerk/DE*; further referred to as powder C2) were used for the coarse fraction. For the fine fraction of the powder compacts, a reactive alumina (CT 3000 SG, *Almatis/DE*; further referred to as powder F1) and an α-Al_2O_3 (AES-41, *Sumitomo/JP*; further referred to as powder F2).

All powders used were sieved through a 100 µm sieve before blending with a polymeric binder. The binder content was kept constant at 5 mass-% respective to the powder weight. After weighing, the powder blends were mixed in a shaker mixer (Turbula T2C, *WAB/CH*) for 20 min. All investigated powder compositions are listed in Tab. 1. To investigate the possible density of a powder bed, samples of the powder blends were

Tab. 1 Fractions of powder blends for sintering experiments

Sample	Powder 1	Fraction [mass-%]	Powder 2	Fraction [mass-%]	Powder 3	Fraction [mass-%]
P-C1/100	C1	100	–	–	–	–
P-C1F1/90	C1	90	F1	10	–	–
P-C1F1/80	C1	80	F1	20	–	–
P-C1F1/70	C1	70	F1	30	–	–
P-C1F1/60	C1	60	F1	40	–	–
P-C1F1/50	C1	50	F1	50	–	–
P-C1C2	C1	50	C2	50	–	–
P-C2F1	C2	50	F1	50	–	–
P-C1/C2/F1	C1	25	C2	50	F1	25
P-C1F2	C1	50	F2	50	–	–
P-C2F2	C2	50	F2	50	–	–

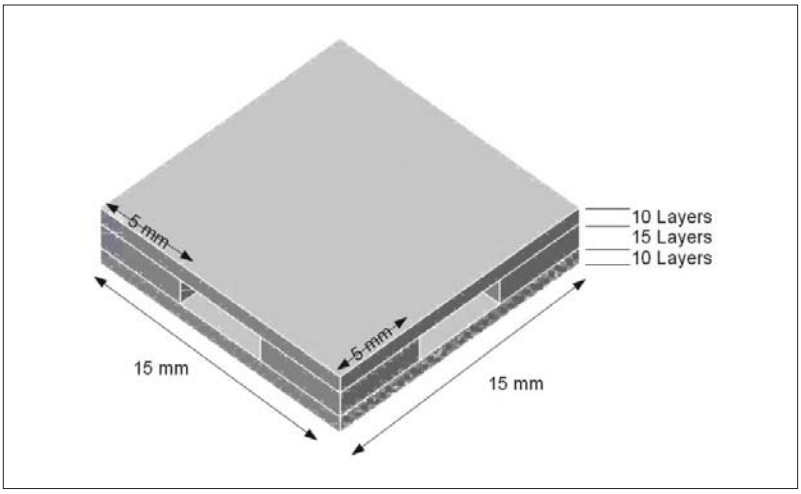

Fig. 9 Construction theme for demonstration parts printed with FuGeMa 1.0

prepared by filling cylindrical porous alumina forms with the mixed powder and smoothing the surface with a doctor blade. The loose alumina powders were sintered at 1600 °C for 120 min or 300 min. After firing, the porosity shrinkage in diameter and density were determined by the Archimedes principle. After measurement, samples were prepared by grinding and polishing and SEM pictures were taken for different magnifications in order to investigate the arrangement of the powder mixtures after sintering.

2.4 Printing of three dimensional demonstration parts with experimental platform

Powder mixtures P-C1/100, P-C1/50 and P-C1/C2/F1 were selected for printing experiments on FuGeMa 1.0. For all three powder compositions, small plates with dimensions of 15 mm × 15 mm and a height of 10 layers were printed. Layer height for those experiments was set to 125 µm. In order to solidify the polymeric binder in selected areas, a binding solution consisting of de-ionized water, ethylene glycol and isopropanol alcohol was used. The binding solution has a viscosity of 1 mPas over the shear rate range from 10 to 1 000 s^{-1} and a surface tension of 39,1 mN/m for a bubble lifetime of 0,5 s. The binding solution was printed with a driving signal of 97 V and 42 µs. For ceramic structures containing no additional dotation with particle-filled inks, the drop distance for the experiments was set to 0,1 mm.

For powder P-C1/C2/F1, also demonstration parts were fabricated. A construction scheme of the demonstration parts is shown in Fig. 9. Parts with layer heights of 100 µm and 125 µm were fabricated.

3 Results and discussion

3.1 Realization of experimental platform for FP-3D

An image of the experimental platform FuGeMa 1.0 is given in Fig. 10. In Fig. 11, part build-up with a generated powder bed for the powder composition P-C1/100 is

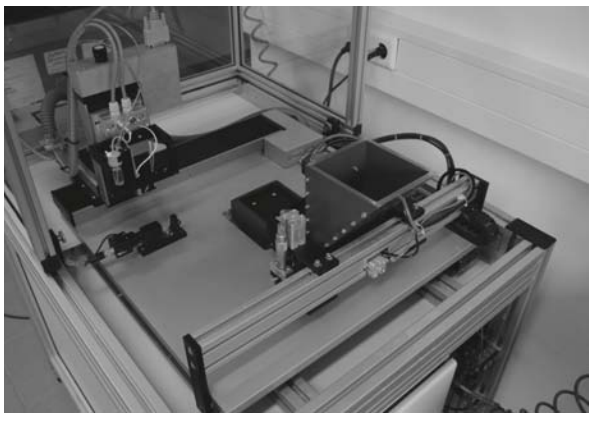

Fig. 10 Experimental platform FuGeMa 1.0 used for printing experiments

Fig. 11 Experimental platform FuGeMa 1.0 during part fabrication

shown. The areas printed can be identified by a slightly darker colour than the rest of the created powder layer.

3.2 Ink characterization and droplet visualization

The values used for calculation and the obtained Ohnesorge numbers are listed in Tab. 2, the viscosities of all inks in dependence of the shear rate applied are illustrated in Fig. 12.

All three inks show slightly shear thinning behaviour. The ink containing alumina and silica shows the biggest decrease in viscosity with increasing shear rate. Starting at 14 mPas the viscosity reaches 9 mPas at high shear. The ink containing silica does nearly not change its viscosity with increased shear. Values obtained for shear rates lower than 100 s^{-1} is not to be considered representative for a drop ejection process. In fact, in printing very high shear rates up to 1000 s^{-1} are applied [13]. For the used rotational viscosimeter is not suitable for stable measurements at shear rates higher than 1000 s^{-1}, the values obtained at 1000 s^{-1} must be considered representative regarding the process of droplet ejection. Since the slope of all curves obtained decrease with increasing shear forces, the values at 1000 s^{-1} are a good approximation of the state during droplet ejection. The calculated Ohnesorge numbers in Tab. 2 confirm printability for the inks AS and A. For ink S, the range of 0,1 to 1, often identified as suitable for stable droplet ejection [14], was not achieved. This can be deducted to the relatively low viscosity compared to ink AS and A. Since a commercially available suspension was used as the starting material and diluted, the principles of particle stabilization, suspension preparation and the exact composition of the suspension could not be reconstructed. During part fabrication it could be observed that ink S had greater tendencies for nozzle clogging especially with increasing fabrication time. For further experiments it could be reasonable to increase the viscosity and therefore the printability of the ink. Another possibility for the preparation of a silica ink is the selection of silica particles similar to ink AS as a source for silica. Those experiments are on-going investigations, but did not yet produce satisfying results comparable to inks A and AS. Besides externally measurable properties, successful droplet ejection is obviously the most critical factor concerning the inks. Since after measurements ink properties have not been adjusted by adding surfactants or viscosity modifiers, the driving signal of the print heads remains the only parameter available for adjustment of droplet formation. Preliminary experiments have identified 114 V and 46 µs as a suitable starting point for particle-filled inks. Drops of all three inks for this driving signal are shown in Fig. 13. For ink A, a single droplet is already formed using this driving signal. For ink AS, a tail following the main droplet can be observed, ink S forms one main and one satellite droplet. The formation of such satellite drops has been reported for inks with low

Tab. 2 Ink properties and Ohnesorge numbers for investigated inks

Ink	Density [g/cm³]	Viscosity [mPas]	Surface tension [mN/m]	Ohnesorge number
Ink AS	1,18	9,1	40	0,1325
Ink A	1,14	8,5	39,4	0,1268
Ink S	1,16	3,4	41,6	0,0489

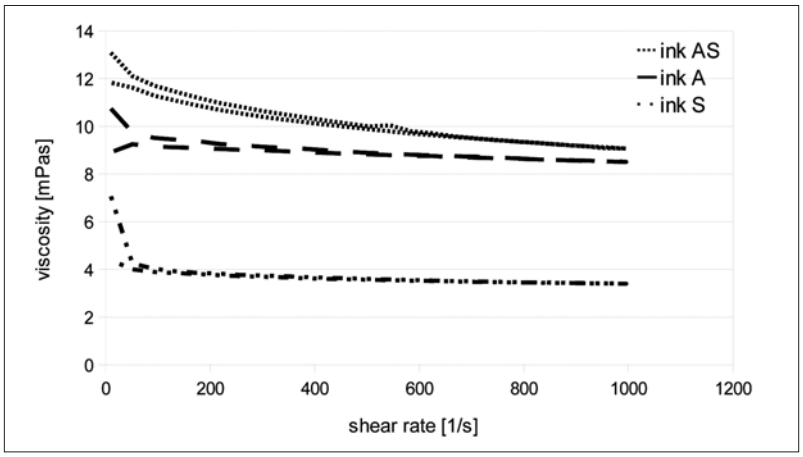

Fig. 12 Viscosity dependency from shear rate for inks A, S, and AS

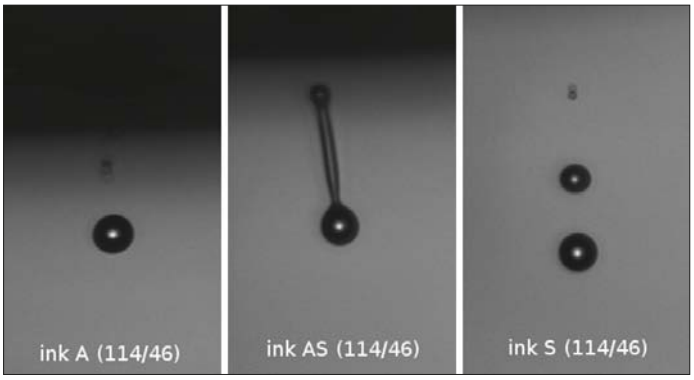

Fig. 13 Drop formation for fixed driving signal 114 V and 46 µs (each drop frame is 700 µm in heigth and 400 µm in width)

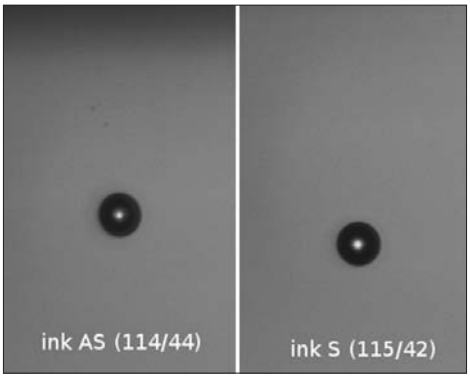

Fig.14 Drop formation with adjusted driving signals for inks AS and S (signal given in picture, 700 µm height and 400 µm width)

Tab. 3 Density, porosity and diameter shrinkage of investigated powder after firing at 1600 °C

Sample	Sintering time at 1600 °C [min]	Density [g/cm³]	Porosity [%]	Diameter shrinkage [%]
P-C1/100	120	1,869	45,83	0
	300	1,902	51,34	0
P-C1F1/90	120	1,577	58,75	0
	300	1,774	54,85	2,7
P-C1F1/80	120	1,525	60	0
	300	1,646	57,69	3
P-C1F1/70	120	1,559	60	1,3
	300	1,588	59,62	3,2
P-C1F1/60	120	1,549	59,62	4,9
	300	1,58	59,57	9,1
P-C1F1/50	120	1,733	56,08	12,9
	300	1,739	55,69	15,1
P-C2	300	2,279	42,105	9,8
P-C1C2	300	1,825	52,67	2,8
P-C2F1	300	1,835	54,4	19,1
P-C1/C2/F1	300	1,894	51,06	15
P-C1F2	300	1,82	53,93	12,9
P-C2F2	300	2,165	45,02	22,6

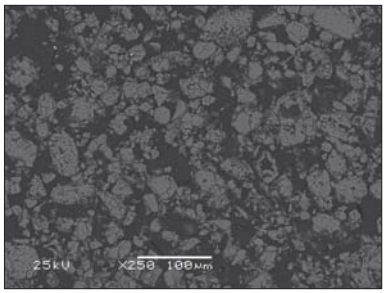

Fig. 15 SEM image of P-C1F1/50 (BSE,250×)

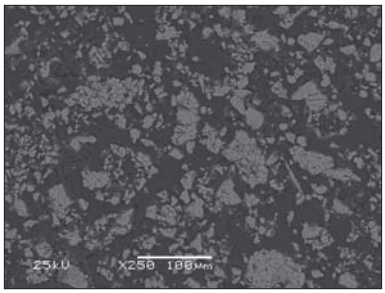

Fig. 16 SEM image of powder P-C1/100

Ohnesorge numbers [15]. All three main droplets have a diameter of around 75 µm for this driving signal. Since surface tensions are very similar for all three inks, the differing drop formation can be attributed to viscosity differences in the inks. Seeing viscosity as a force hindering fluid movement caused by shear forces, drop breakup from the nozzle tip is hindered by high viscosities of the ink. For the ink with the highest viscosity (ink AS), drop breakup from the nozzle tip is delayed and therefore a tail occurs after the droplet. For the low viscosity ink (ink S), the same signal causes two droplets to be ejected because forces hindering fluid movement are significantly lower. The formation of drops from print heads has been studied by numerous researchers (i.e. [16–19]) but the variety of fluid properties, print head designs; signal shapes or drop formation mechanisms investigated complicate the drawing of universally valid rules for successful drop formation. The Ohnesorge number is one of the criteria most researches refer to. Since drop formation is one aspect of the process studied here, a more experimental approach seems to be more purposeful in this case. Experiments show that slight changes in the driving signal enable the formation of single droplets with all three inks. For ink A, the signal remained unchanged since 114 V/46 µs already produced a single droplet. The changed signals and corresponding drops formed for inks AS and S are given in Fig. 14.

3.3 Powder selection

The values of density and porosity for the investigated powders are given in Tab. 3. In most cases porosity of the powder compacts is higher than 50 %. Only P-C1/100 and P-C2F2 have porosities lower than 50 %. In case of P-C1/100, the measured density does not exceed 1,9 g/cm³. The density of the samples measured is increased with holding time, the biggest increase is obtained for P-C1F1/90 with 0,197 g/cm³. For all samples except P-C1/100, where porosity increased with holding time, the porosity is decreased, the density increased and the shrinkage increased by changing the holding time from 120 min to 300 min. The tabular alumina used for C1 shows nearly no reactivity at 1600 °C, but still the highest density value for all blends of C1 and F1 is obtained after firing. For it is not caused by densification at high temperatures, the high density must originate from a higher particle packing density in the prepared sample before firing. Increasing the density of powders has been of great interest to the ceramic industry for many decades. Numerous models for calculating and optimizing particle densities have been developed, a majority based on the models developed by *Furnas* [20] and *Andreasen* [21]. By mixing multiple fractions of discrete particle sizes at defined ratios, the smaller fractions occupy the space left in the package of the coarse fractions. The efficiency of packing is determined by sizes, size distributions and shape of the powders used. While the packing densities increase through such measures for powders with rather big particle sizes, for fine particles inner friction of the particles increases through a higher specific surface area and interparticluar forces, such as electrostatic and van der Waals forces, increase agglomeration and prevent a density increase [22]. Fig. 15 shows a SEM image of powder mixture P-C1F1/50. The fine particles of fraction F1 have either adhered to the coarse and irregular shaped grains of fraction C1 (shown in Fig. 16) or formed agglomerates of highly spherical shape, leading to loosening of powder C1 and to decreasing the density of the initial powder packing before firing. Due to the high reactivity of F1, the shrinkage in samples containing C1 and F1 increases with the content of F1 (see Tab. 3). At 50 mass-% F1, the high reactivity and densification rate of F1 compensates for the lack

Fig. 17 Demonstration parts printed with custom 3DP machine (layer height 125 µm); left: as-printed; right: sintered

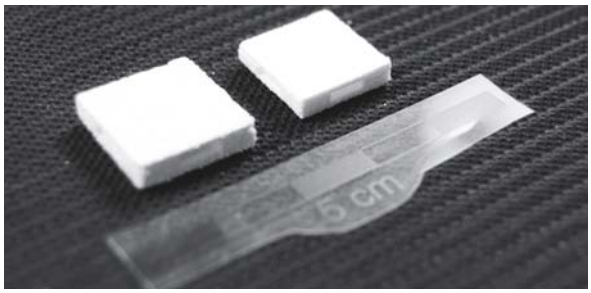

Fig. 18 Demonstration parts printed with custom 3DP machine (layer height 100 µm); left: as-printed; right: sintered

of packing density thus increasing the density compared to samples containing smaller fractions of F1. Analogous tendencies can be observed for powder C2. Being a granulated alumina powder with high sphericity and high reactivity compared to C1, it shows higher shrinkage and density and lower porosity. Adding finer particles to C2 does not increase density of the obtained compacts but shrinkage is increased due to higher reactivity of components F1 and F2. But with such large particle sizes for C2, the printing process must ensure a high impact range in order to bind the spread particles during printing. This would need an increased saturation with binding solution which is leading to dimensional intolerance in the resulting parts.

The investigation was aiming at increasing the mechanical stability of samples fabricated with the experimental platform since prior experiments revealed that samples have insufficient strength for proper handling and further testing [5]. Since online testing of the powder layers is not possible without destructing the particle arrangement present in the powder layer, comparing powder mixtures after sintering can provide a good comparative basis for the selection of raw materials and blends thereof. Increased densities in loose powder bulks are likely to lead to higher densities in printed parts. The experiments conducted here indicate that the use of a singular powder offers the best chances of obtaining a compact with sufficient mechanical strength. But due to the need for binder saturation (powder C2) or low reactivity (C1) it is not likely to obtain dimensionally correct of mechanically stable parts from using singular powders. Still, the metering with vibration and compaction by the doctor roller in the process can lead to differing results and changed particle arrangements in the printed parts due to compensation of inner friction between fine particles and thus preventing agglomeration phenomena discussed above. For this reason, powder mixtures of fine and coarse particles still offer the best compromise between packing density, moderate shrinkage, resulting density and part properties.

3.4 Fabrication of demonstration parts

An illustration of produced demo parts before and after sintering at 1600 °C is given in Fig. 17 and 18. Fig. 17 shows a part with a layer height of 125 µm, Fig. 18 a part with 100 µm layer height. On each figure, the part before sintering is shown on the left side, the fired part is shown on the right. In order to determine printing accuracy and part shrinkage, the part dimensions were measured before and after sintering. The images show, that the channels build into the parts remain intact and permeable after sintering. The stresses arising during firing are not critical for the wall thickness produced in these parts. In x and y dimensions the parts have an average length of 15,08 mm in x and 15,19 mm in y with a standard deviation of 0,02 in x and 0,02 in y for the parts produced with 100 µm layer height, and 15,10 mm in x and 15,21 mm in y with a standard deviation of 0,12 mm in x and 0,08 mm in y for the parts with 125 µm layer height. In z direction the parts with 100 µm layer height have an average of 4,02 ± 0,04 mm, for 125 µm layer height the average is 4,95 ± 0,01 mm. With the desired dimensions of the parts being 15 mm × 15 mm in x and y and 3,5 mm (for 100 µm layer height) and 4,375 mm (125 µm layer height) it can be stated that the x and y dimensions are matched quite well whereas the z direction is significantly larger than given by the printing data. This elongation can be credited to the penetration of binding solution into the powder bed. The penetration depth of the binding solution exceeds the set layer height leading to binding of thicker areas than desired by the data design. One approach to eliminate such effects is the reduction of binder saturation in the powder bed during printing. Experiments prior to the printing test have indicated that lower binder saturation as chosen for the experiments shown does not suffice to create an interlayer binding of the powder bed within the parts. The parts cannot be dismantled from the loose powder bed without damage. A similar problem was investigated by *Moon et al.* [23]. The infiltration kinetics of high molecular weight binder into a powder bed for slurry-based 3DP were analysed and the authors state that besides powder bed characteristics, surface tension and viscosity of the binder mostly determine the infiltration kinetics. Low surface tension of the binder results in big spreading of the binder droplet and reduced infiltration into the powder bed, higher viscosity results in higher dimensional accuracy in plane but lower infiltration depth as well. Since the binding solution used here has a very low viscosity of 1 mPas, increasing the viscosity of the binder combined with slightly higher surface tensions could path a way to achieving smaller infiltration depths without compromising the dimensional accuracy in the printing plane thus creating the ability to gain control of the z dimension in the same fashion as x and y. The shrinkage in the demonstration parts was measured to an average of 9,3 % in the printing plane (100 µm layers) respectively to 10,2 % (125 µm layers). The shrinkage in the z direction was determined to be 11,6 % (100 µm layers) respectively 13,5 % (125 µm layers). Due to the layered structure of the parts the grains from powder component C1 with irregular shapes have been known to orientate in the processing direction, which here is the printing plane. The spherical grains incorp-

orated in the powders are not known to cause anisotropy in shrinkage. The irregular shaped grains are oriented along the printing plane therefore causing higher shrinkage in the z direction of the parts.

4 Conclusions and Outlook

While in former publications the preparation of suitable inks and the selective doping of ceramic structures in three dimensions on a newly developed experimental platform (FuGeMa 1.0) for a new process based on three dimensional printing methods has been established in principle, this paper focusses on the printability of prepared inks and the optimization of the powder bed necessary for part generation. Prepared inks are characterized regarding viscosity, density and surface tension and the printability is judged by the use of the Ohnesorge number. For the creation of single droplets during the printing process is effected by part properties as well as the driving signal of the print heads, it is suggested to consider the Ohnesorge number a good indicator for ink printability while favouring an experimental approach to the adjustment of the print head driving signal for forming stable single droplets. Investigations for powder raw materials suitable for the developed process reveal that the particle sizes chosen especially for the fine fractions are to small for acting as a filler for the voids left by the coarse powders used. Due to inter-particular forces agglomeration is caused leading to minor properties regarding density and porosity, neglecting principles and formulas consistent for powders with significantly lager particle sizes. But due to process related restrictions and desired part characteristics like the need for dimensional accuracy and sufficient mechanical stability, mixtures of coarse and fine particles still have to be favoured for use in functional printing in three dimensions. The influence through powder metering by vibration and the use of a compaction roller for powder layer generation is likely to reduce inner friction of the particles, to decrease tendency for agglomeration and to produce denser powders layer compared to the experiments performed detached from the process. Developing analytical solution for monitoring powder bed properties during the process arises as a topic of great interest and is therefore the subject of current research. Parts fabricated with powder mixtures on the experimental platform show promising dimensional accuracy and suitable properties after firing, leaving great promise for combining part fabrication and local doping in the near future.

By obtaining tools and approaches for process realization, data processing, ink selection, powder selection, doping of selected regions during printing and part fabrication from former and the presented research, combining those findings is the next and already on-going development step for the realization of locally doped ceramic parts from Functionalized Printing in Three Dimensions (FP-3D).

Acknowledgements

The authors gratefully acknowledge support for this research from the *German Research Foundation,* funded this study in *SPP 1418 "FIRE"* under the number KO 898/9-1.

References

[1] Joliff, Y.; Absi, J.; Glandus, J. C.; Huger, M.; Tessier-Doyen, N.: Experimental and numerical study of the thermomechanical behaviour of refractory model materials. Journal of the European Ceramic Society 27 (2007) [2-3]. 1513–1520.

[2] Aneziris, C. G.; Geigenmüller, A.: Feuerfest und schadstoffarm. forschung - Mitteilungen der DFG 35 (2010) [S1]. 10–15.

[3] Kollenberg, W.: Keramische Komponenten mit variablem Mikrogefügedesign. (2010) DE 10 2008 028 742 B4 17.06.2008.

[4] Polsakiewicz, D.; Kollenberg, W.: Generativ hergestellte keramische Bauteile mit dreidimensional funktional-gradierten Strukturen. DKG-Jahrestagung. 22.-24.3-2010. Hermsdorf.

[5] Polsakiewicz, D.; Kollenberg, W.: Improvement of thermo shock performance by three dimensional graded structures. Proceedings of the 54th International Conference on Refractories 2011 in Aachen.

[6] Polsakiewicz, D. A.; Kollenberg, W.: Highly loaded alumina inks for use in a piezoelectric print head. Mat.-wiss. u. Werkstofftech 42 (2011) [9]. 812–819.

[7] Utela, B.; Storti, D.; Anderson, R.; Ganter, M.: A review of process development steps for new material systems in three dimensional printing (3DP). Journal of Manufacturing Processes 10 (2008) [2]. 96–104.

[8] Sachs, E.; Wylonis, E.; Allen, S.; Cima, M.; Guo, H.: Production of injection molding tooling with conformal cooling channels using the three dimensional printing process. Polym Eng Sci 40 (2000) [5]. 1232–1247.

[9] Yang, S.; Evans, J. R. G.: Metering and dispensing of powder; the quest for new solid freeforming techniques. Powder Technology 178 (2007) [1]. 56–72.

[10] Calvert, P.: Inkjet Printing for Materials and Devices. Chem. Mater. 13 (2001) [10]. 3299–3305.

[11] Mott, M.; Song, J.-H.; Evans, J. R. G.: Microengineering of Ceramics by Direct Ink-Jet Printing. Journal of the American Ceramic Society 271 (1999) [7]. 1653–1658.

[12] Zhao, X.; Evans, J. R. G.; Edirisinghe, M. J.; Song, J. H.: Ink-jet printing of ceramic pillar arrays. Journal of Materials Science 37 (2002) [10]. 1987–1992.

[13] Ramakrishnan, N.; Rajesh, P. K.; Ponnambalam, P.; Prakasan, K.: Studies on preparation of ceramic inks and simulation of drop formation and spread in direct ceramic inkjet printing. Journal of Materials Processing Technology 169 (2005) [3]. 372–381.

[14] Özkol, E.; Ebert, J.; Telle, R.: An experimental analysis of the influence of the ink properties on the drop formation for direct thermal inkjet printing of high solid content aqueous 3Y-TZP suspensions. Journal of the European Ceramic Society 30 (2010) [7]. 1669–1678.

[15] Jang, D.; Kim, D.; Moon, J.: Influence of Fluid Physical Properties on Ink-Jet Printability. Langmuir 25 (2009) [5]. 2629–2635.

[16] Reis, N.; Ainsley, C.; Derby, B.: Ink-jet delivery of particle suspensions by piezoelectric droplet ejectors. Journal of Applied Physics 97 (2005) [9]. 94903.

[17] Dong, H.; Carr, W. W.; Morris, J. F.: An experimental study of drop-on-demand drop formation. Physics of Fluids 18 (2006) [7]. 72102.

[18] Dong, H.; Carr, W. W.; Morris, J. F.: Visualization of drop-on-demand inkjet: Drop formation and deposition. Review of Scientific Instruments 77 (2006) [8]. 85101.

[19] Xu, Q.; Basaran, O. A.: Computational analysis of drop-on-demand drop formation. Physics of Fluids 19 (2007) [10]. 102111.

[20] Furnas, C. C.: Grading Aggregates - I. - Mathematical Relations for Beds of Broken Solids of Maximum Density. Ind. Eng. Chem 23 (1931) [9]. 1052–1058.

[21] Andreasen, A.: Über die Beziehung zwischen Kornabstufung und Zwischenraum in Produkten aus losen Körnern (mit einigen Experimenten). Colloid & Polymer Science 50 (1930) 217–228.

[22] Yu, A. B.; Bridgwater, J.; Burbidge, A.: On the modelling of the packing of fine particles. Powder Technology 92 (1997) [3]. 185–194.

[23] Moon, J.; Grau, J. E.; Knezevic, V.; Cima, M. J.; Sachs, E. M.: Ink-Jet Printing of Binders for Ceramic Components. Journal of the American Ceramic Society 85 (2002) [4]. 755–762.